International Journal of Engineering Innovation & Research
Volume 5, Issue 1, ISSN: 2277 – 5668

A Combined Structural and Electromechanical Approach for Vibration Attenuation of Rotating Beam

Ali Gerami, Majid Dousti, Saeid Dousti

***Abstract* – Piezoelectric materials (PZT) have been used in the past to reduce the vibration in several different applications. This paper takes a combined structural and electromechanical approach to reduce the vibration amplitude of a rotating cantilever beam. This yields to a coupled electro-mechanical system, wherein displacement variables are coupled via electric field. Due to the rotation of the beam, the centrifugal stiffening effect is also included in the derivation. A linear partial differential equation is derived from the Hamilton's principle, which later solved to study the natural frequencies and the tip response of the beam. Several parametric studies including rotational speed of beam, beam thickness, hub radius and shunt resistance were also conducted. A resistive circuit was later connected to the piezoelectric pieces in series and was tuned to reduce the vibration in a wide frequency range. A good broadband vibration reduction was achieved by tuning each shunted circuit to a different target frequency.**

***Keywords* – Piezoelectric, Periodic Structure, Transfer Matrix, Rotating Structure.**

I. INTRODUCTION

Rotating beams are found in several engineering designs such as turbine blades and aircraft rotary wings. Since structural vibration can potentially reduce the life expectancy and the performance of the structure, vibration attenuation is desirable in many engineering applications. Vibration attenuation can be achieved by using active or passive materials. Passive materials convert the structural deformation to thermal energy; while active materials cant react to the deflection in a controlled manner to diminish the vibration [1].

Beams with periodic piezoelectric arrays have attracted more and more attention in recent years. These beams are conventionally designed for wave propagation and vibration attenuation. Piezo-materials are transformers that convert mechanical energy into electrical energy and vice versa. When they are bonded to a structure, the mechanical energy absorbed in the piezo-material is converted to electrical voltage in the poling direction of the piezo-material device. Equally spaced piezo-actuators introduce periodicity into the system that can also help reducing the vibration in the structure's stop bands. Extensive research has been done on wave propagation in periodic structures. Orris [2] used Finite element method to calculate the frequency response of a periodic beam. Shen [3] conducted a mathematical study to identify the Eigen-function solution of a rotating periodic structure, more specifically a rotating plate. Duhamel [4] used a combination of wave and finite element analysis to determine the forced response of a rotating structure and proved the efficiency of the combined approach by comparing his results with the former mathematical models. Romeo [5] analyzed the response of a non-rotating periodic beam to harmonic excitation. The wave propagation method was used in the study to avoid numerical difficulties that arise in solving the problem using the transfer matrix formulation. Polach [6] used finite element method to calculate the natural frequencies and mode shapes of a rotating periodic structure and applied the method to rotating turbine blades by mathematically dissecting the turbine disk into identical parts. The introduction of an external R-L shunt circuit forms a resonance with the piezoelectric capacitance and the frequency of this RLC circuit can then be tuned to eliminate or reduce the vibration in target the frequencies. Vibration suppression using piezoelectric pairs has been investigated in many cases. Thorp [7] used piezoelectric actuators with passively shunted resistors that were

Nomenclatures

A	Area of the PZT perpendicular to the poling direction
C_{el}	Electrical damping matrix
C_p	Capacitance matrix
M_{el}	Electrical mass matrix
d_{31}	Original piezoelectric coupling coefficient
$d(t)$	Temporal coordinates for electrical degrees of freedom
$r(t)$	Temporal coordinates for mechanical degrees of freedom
D	Electrical displacement
e	Coupling coefficient
E	Electric field
K	Kinetic energy
$K_{Dynamic}$	Dynamic stiffness
R	Shunt resistance
S	Strain of the beam elements
T	Stress in the beam elements
u	Displacement
U	Potential energy
V	Volume of the element
W	External work done on the system
Greek Symbols	
ε	Dielectric constant
ρ	Density of the Piezoelectric material
ω	Excitation frequency
Ψ	Electrical shape function of the piezoelectric element
φ	Mechanical shape function of the piezoelectric element
Θ	Electromechanical coupling matrix

periodically placed along a beam to control the longitudinal wave propagation. The resulting periodic structure was capable of filtering the propagation of waves over specified frequency bands called the stop bands. Similar studies have been done by Ruzzene [8,9], Hangood [10], and Kandagal [11]. Other researchers such as Singh [12] actively controlled a periodic structure by piezoelectric patches to reduce vibration of the system. Tang [13] used a combination of actively controlled and passively shunted piezoelectric actuators to control the vibration of a rotating periodic structure. The combined approach helped reducing the control effort and therefore the energy consumption while maintaining the necessary vibration control. Kaufman [14] employed a semi-active method to reduce the vibration in turbo-machinery blades with a variable rotating speed and therefore achieved a longer lifetime for the blades. Zhou [15] achieved vibration reduction in a large bandwidth by using high order shunt circuits but as expected a smaller amplitude reduction was achieved by using this method. Same procedures were used to reduce the unwanted vibration of plates. Studies done by Spadoni [16] and Becker [17] are a few examples. Other interesting applications of the concept include: noise reduction in heavy-duty trucks (Raju & Bianchini [18]), hybrid composites (Alderaihem et al. [19]), and space structures (Hagood et al. [20]).

In this paper the transfer matrix methods is used due to its accuracy and a passive approach with focus on utilizing the periodicity of the structure for vibration attenuation is applied over a broad band of frequencies. In contrast to the other research in this paper in order to achieve broadband vibration reduction each piezo-electric patch is tuned to a different target frequency

II. MODELLING

A rotating beam with periodically installed piezoelectric actuators on top and bottom is considered for this study (see Fig. 1). More details and the beam specifications can be found on Section 4. Here a general model for a periodic rotating structure is developed. This model will later on be adapted to the case study presented in this paper.

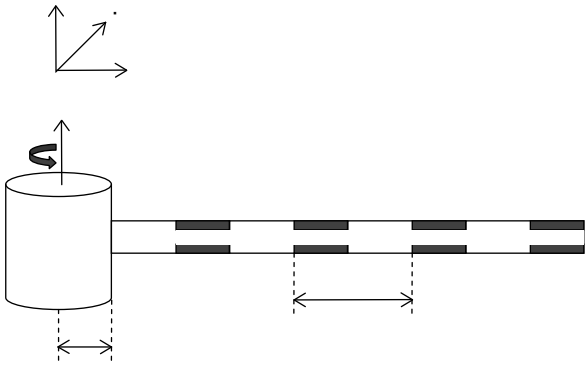

Fig.1. Rotating beam with piezoelectric patches.

Hamilton's principle is used to derive the dynamic equation of the system:

$$\int_{t_1}^{t_2} (\delta K - \delta U + \delta W)dt = 0 \tag{1}$$

Here, K represents the kinetic energy, U the potential energy and W the external work done on the system.

$$K = \frac{1}{2}\int_{V_s} \rho_s \dot{u}^T \dot{u} dV_s + \frac{1}{2}\int_{V_p} \rho_p \dot{u}^T \dot{u} dV_p \tag{2}$$

$$\begin{aligned} U &= \frac{1}{2}\int_{V_s} S^T T dV_s + \frac{1}{2}\int_{V_p} S^T T dV_p \\ &\quad - \frac{1}{2}\int_{V_p} D^T E dV_p \end{aligned} \tag{3}$$

$$\begin{aligned} \delta W &= \sum_{i=1}^{nf} \delta u(x_i).f_i(x_i) \\ &\quad - \int_0^l f_c(x)\frac{\partial u}{\partial x}\left(\frac{\partial \delta u}{\partial x}\right)dx \\ &\quad + A_S \int_A \delta D(-L\ddot{D} - R\dot{D})dA \end{aligned} \tag{4}$$

The dynamic equation of the piezoelectric actuators is described as:

$$\begin{bmatrix} T \\ D \end{bmatrix} = \begin{bmatrix} c^E & -e \\ e & \varepsilon^S \end{bmatrix} \begin{bmatrix} S \\ E \end{bmatrix}, \quad \begin{bmatrix} T \\ E \end{bmatrix} = \begin{bmatrix} b & -h \\ -h & \beta \end{bmatrix} \begin{bmatrix} S \\ D \end{bmatrix} \tag{5}$$

Where;

$$\beta = \frac{1}{\varepsilon^s} \qquad h = \frac{e}{\varepsilon^s} \qquad b = c^E + \frac{e^2}{\varepsilon^s} \tag{6}$$

Here, T is the stress on the piezo patch, D is the electric displacement, c is the elasticity, e is the piezoelectric coupling, ε is the electric constant. S is the dimensionless deflection of the patch (strain), E is the electric field, the superscript, E, indicates that the parameter was measured at constant electric field and the superscript, S, signifies that the parameter was measured at constant strain. This equation introduces the piezoelectric electromechanical interaction into the model. The piezoelectric coupling coefficient (e) relates the mechanical stress in the patch to the applied electric field. This coupling coefficient can also be written with the use of the more familiar coupling coefficient d_{31} as presented in Eq. (7):

$$e = d_{31}c^E \tag{7}$$

For the piezoelectric coupling coefficient d_{31}, the subscripts '1' and '3' refer to the direction of the applied field and the poling direction, respectively. Introducing the piezoelectric material properties Eq (5) into Eq. (3):

$$U=\frac{1}{2}\begin{vmatrix}\int_{V_s} c_s S^T S dV_s+\int_{V_P} bS^T S dV_P\\ -\int_{V_P} hS^T D dV_P+\int_{V_P} hD^T S dV_P\\ +\int_{V_p} \beta D^T D dV_p\end{vmatrix} \quad (8)$$

Equations 2 and 8 can be written in variational form as follows:

$$\begin{aligned}\delta U=&\int_{V_s} c_s \delta S^T S dV_s+\int_{V_P} b\delta S^T S dV_P-\\&-\int_{V_P} h\delta S^T D dV_P+\int_{V_P} h\delta D^T S dV_P\\&-\int_{V_P} \beta\delta D^T D dV_P\end{aligned} \quad (9)$$

$$\delta K=\int_{V_s} \rho_s \delta\dot{u}^T \dot{u} dV_s+\int_{V_P} \rho_P \delta\dot{u}^T \dot{u} dV_P \quad (10)$$

Substituting Eqs. (9) and (10) into Eq. (1):

$$\int_{t_1}^{t_2}\begin{bmatrix}\int_{V_s} \rho_s \delta\dot{u}^T \dot{u} dV_s+\int_{V_P} \rho_P \delta\dot{u}^T \dot{u} dV_P\\ -\int_{V_s} c_s \delta S^T S dV_s-\int_{V_P} b\delta S^T S dV_P\\ +\int_{V_P} h\delta S^T D dV_P-\int_{V_P} h\delta D^T S dV_P\\ +\int_{V_P} \beta\delta D^T D dV_P+\sum_{i=1}^{nf}\delta u(x_i) f_i(x_i)\\ -\int_0^l f(x)\frac{\partial u}{\partial x}\left(\frac{\partial \delta u}{\partial x}\right)dx\\ +A_s\int_A \delta D\left(-L\ddot{D}-R\dot{D}\right)dA\end{bmatrix} dt=0 \quad (11)$$

It is necessary to make a few simplifying variables before attempting to solve Eq. (11). The displacement of the beam can be written as follows:

$$u(x,t)=\varphi(x)r(x) \quad (12)$$

Where row vector $\varphi(x)$ is the assumed to be the mechanical shape function of the piezoelectric element and $r(t)$ is the temporal coordinates for mechanical degrees of freedom. According to Euler–Bernoulli beam theory, strain in the beam is the product of the distance from the neutral axis and the second derivative of displacement with respect to the position along the beam. Therefore, the following equation can be used to define the strain:

$$S=-y\frac{\partial^2 u(u,t)}{\partial x^2}=-y\varphi(x)'' r(t) \quad (13)$$

The electrical displacement can be written as:

$$D(x,t)=\varphi(x)d(t) \quad (14)$$

Where row vector $\psi(t)$ is the electrical shape function of the piezoelectric element and $d(t)$ is the temporal coordinates for the electrical degrees of freedom.

The case under consideration in this study is a beam with bimorph piezoelectric material elements on its top and bottom as shown in Figure (1). In this Figure 'a' is the hub radius.

Using Eqs (12), (13), and (14) leads to a simplified equation of motion. The mass and stiffness matrices are as follows:

$$M_s=\int_{V_s}\rho_s\varphi^T(x)\varphi(x)dV_s \quad (15)$$

$$M_P=\int_{V_P}\rho_P\varphi^T(x)\varphi(x)dV_P \quad (16)$$

$$K_s=\int_{V_s} y^2 c_s\varphi^T(x)''\varphi(x)'' dV_s \quad (17)$$

$$K_P=\int_{V_P} y^2 c\varphi^T(x)''\varphi(x)'' dV_P \quad (18)$$

$$K(Rot)_s=\int_{V_s} f\varphi^T(x)''\varphi(x)'' dV_s \quad (19)$$

$$K(Rot)_P=\int_{V_P} f\varphi^T(x)''\varphi(x)'' dV_P \quad (20)$$

The electromechanical coupling matrix Θ and the capacitance matrix C_p are defined as:

$$\Theta=-\int_{V_P} yh\varphi^T(x)''\psi(x)'' dV_P \quad (21)$$

$$C_P=-\int_{V_P}\beta\psi^T(x)''\psi(x)'' dV_P \quad (22)$$

Electrical mass matrix (M_{el}) and electrical damping (C_{el}) matrix are as follows:

$$M_{el}=\int_{A_P} A_s L\psi^T(x)\psi(x)dA_P \quad (23)$$

$$C_{el}=\int_{A_P} A_s R\psi^T(x)\psi(x)dA_P \quad (24)$$

Substituting the parameters defined in Eqs. (15) to (24) into Eq. (11):

$$\int_{t_1}^{t_2}\begin{bmatrix}\delta\dot{r}^T(t)(M_s+M_p)\dot{r}(t)\\ -\delta r^T(t)\begin{pmatrix}K_s+K_p+K(Rot)_s\\ +K(Rot)_P\end{pmatrix}r(t)\\ +\delta r^T(t)\Theta d(t)-\delta d^T(t)\Theta^T r(t)\\ -\delta d^T(t)C_p d(t)\\ -\delta d^T(t)M_{el}\ddot{d}(t)-\delta d^T(t)C_{el}\dot{d}(t)\\ +\sum_{i=1}^{nf}\delta r(t)\varphi(x_i)^T f_i(t)\end{bmatrix} dt=0 \quad (25)$$

Integration of the equation produces the following two coupled equations, which are coupled by the electromechanical coupling matrix Θ. Eq. (26) defines the mechanical motion and Eq. (27) defines the electrical properties of the system:

$$\begin{aligned}&(M_s + M_p)\ddot{r}(x)\\&+(K_s + K_p + K(Rot)_s + K(Rot)_p)r(t)\\&-\Theta d(t) = \sum_{i=1}^{nf}\varphi(x_i)^T f_i(x)\end{aligned} \quad (26)$$

$$M_{el}\ddot{d}(t) + C_{el}\dot{d}(t) + C_p d(t) + \Theta^T r(t) = 0 \quad (27)$$

Eqs. (26) and (27) represent the proposed electro-mechanical system and can be used to determine the motion of the beam. The two equations can be combined as:

$$\begin{aligned}&\begin{bmatrix} M_s + M_p & 0 \\ 0 & M_{el}\end{bmatrix}\begin{bmatrix}\ddot{r}(t)\\ \ddot{d}(t)\end{bmatrix} + \begin{bmatrix}0 & 0\\ 0 & C_{el}\end{bmatrix}\begin{bmatrix}\dot{r}(t)\\ \dot{d}(t)\end{bmatrix}\\&+\begin{bmatrix}K_s + K_p + K(Rot)_s + K(Rot)_p & -\Theta\\ \Theta^T & C_P\end{bmatrix}\begin{bmatrix}r(t)\\ d(t)\end{bmatrix}\\&=\begin{bmatrix}\sum_{i=1}^{nf}\varphi(x_i)^T f_i(t)\\ 0\end{bmatrix}\end{aligned} \quad (28)$$

In this paper, the beam is composed of 3 identical sections. Each section has a pure beam element on the left and a beam element with a piezoelectric patch on the right. Eq. (28) is the equation of motion of the rotating piezo-element on the right. The equation of motion for the left side element (element without piezo patches) can be written as:

$$[M_s][\ddot{r}(t)] + [K_s + K(Rot)_s][r(t)] = \sum_{i=1}^{nf}\varphi(x_i)^T f_i(t) \quad (29)$$

By assembling these element matrices into a global matrix and solving for the above equations the tip response and the natural frequencies of the model can be obtained.

III. Solution Method

In order to calculate the natural frequencies of the beam, first the element matrices must be assembled to obtain the structural mass [M] and stiffness [K] matrices. The natural frequencies can found from the following:

$$\begin{aligned}&[K_{Dynamic}]\{u\} = 0\\&K_{Dynamic} = K - \omega^2 M\end{aligned} \quad (30)$$

Where, $K_{Dynamic}$ is the dynamic stiffness matrix. In order to enforce the boundary conditions using matrix partitioning, the first two rows and columns of the structure's dynamic stiffness matrix should be eliminated. The boundary conditions are the cantilever boundary conditions. Later the forced response can be obtained from:

$$[K_{Dynamic}(\omega)]\{u\} = \{F\} \quad (31)$$

Where $\{F\}$ is the vector of externally applied forces and ω is the excitation frequency. In an other form:

$$\{u\} = [K_{Dynamic}(\omega)]^{-1}\{F\} \quad (32)$$

For all the cases presented in the next section, the excitation force is applied to the root of the beam (second node) and the vibration amplitude is measured at the tip of the beam (last node). Transfer function amplitude is the logarithmic ratio of vibration amplitude at the end to vibration amplitude at the root of the beam:

$$Trasfer\ matrix\ amplitude = 20 \times \log\left(\frac{A(l_n)}{A(l_2)}\right) \quad (33)$$

In which, $A(l_2)$ and $A(l_n)$ are vibration amplitude in the second and the last node consequently.

IV. Results and Discussions

As a case study, a slender cantilever beam with 4 identical cells was modeled using the proposed method in section 2. A pair of piezoelectric patches is embedded symmetrically at the top and bottom surfaces of the right hand side element of each cell. Later, a sinusoidal load was applied at the root of the beam. In order to demonstrate the effect of the structure's periodicity, the uniform beam was used as a benchmark (Fig. (2)).

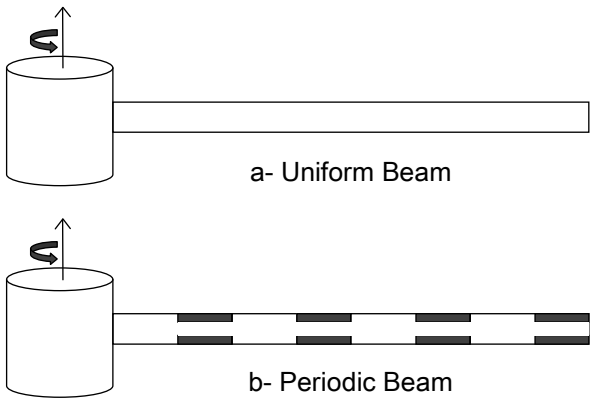

Fig. 2. Different beam cases investigated.

The beam is made of aluminium with specifications demonstrated in Table 1.

Table 1. Model Specifications.

Parameter	Value	Unit
Beam length	0.45	m
Beam width	0.036	m
Beam height	0.003	m
Modulus of elasticity of the beam	73	Gpa
Density of the beam	2700	Kg/m3
Charge constant	2.37E-8	m/V
Dielectric constant	2.1E-10	F/m
Density of the piezo patch	7700	Kg/m3
Modulus of elasticity of the piezo patch	69	Gpa
Piezo patch length	0.07	m
Piezo patch width	0.036	m
Piezo patch height	0.001	m

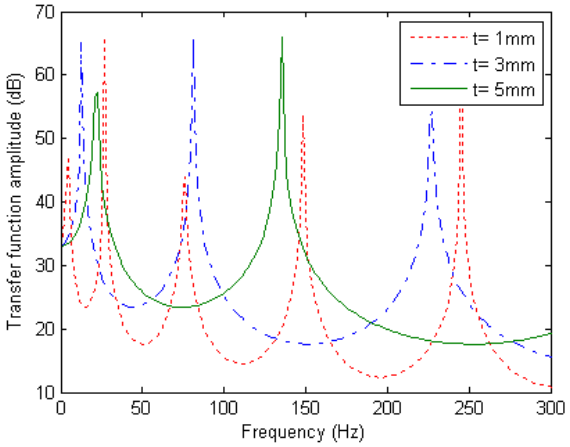

Fig. 3. Uniform beam with different thicknesses.

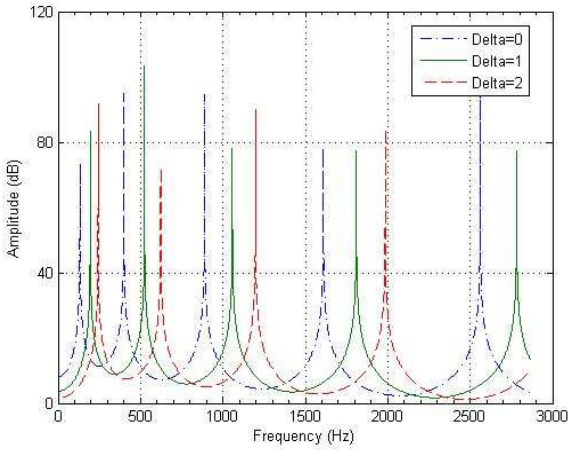

Fig. 4. Uniform beam with different hub radiuses.

Some parametric studies including change in beam thickness, hub radius and rotational speed are investigated and consequently reported in Figures 3, 4, and 5. Due to the increase in rotational speed, the rotational stiffness grows which cases a shift in the natural frequencies toward higher frequencies. Augmentation of hub radius affects the natural frequencies of the rotating beam in the same manner. In addition an increase in thickness results in higher stiffness and higher natural frequencies as well.

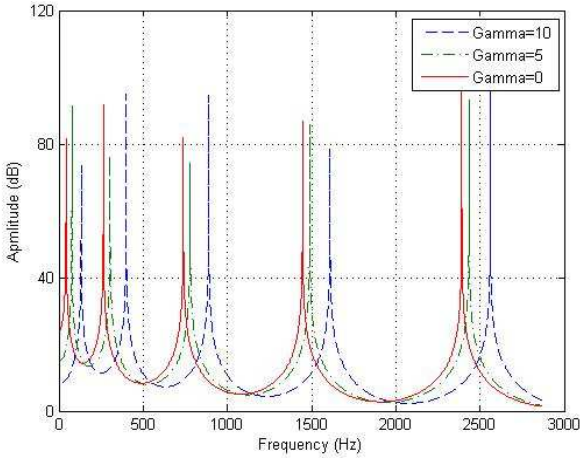

Fig. 5. Uniform beam with different rotational speeds.

In order to achieve the vibration suppression in a specified frequency band, shunt circuit resonant frequencies should be tuned to natural frequencies of the beam at that band. While broadband vibration suppression can be achieved by setting the tuning frequencies to several different natural frequencies of the beam, narrow band vibration reduction can be obtainable by setting all tuning frequencies to a specific natural frequency. A change in shunt circuit resistance causes a dramatic change in tip response of the beam. The effect of shunt resistance on the beam's frequency response and the optimal resistance is displayed in Figure 6. In this figure the tuning frequency was set to 570 Hz and the resistance was changed from 400 to 1200 Ohm.

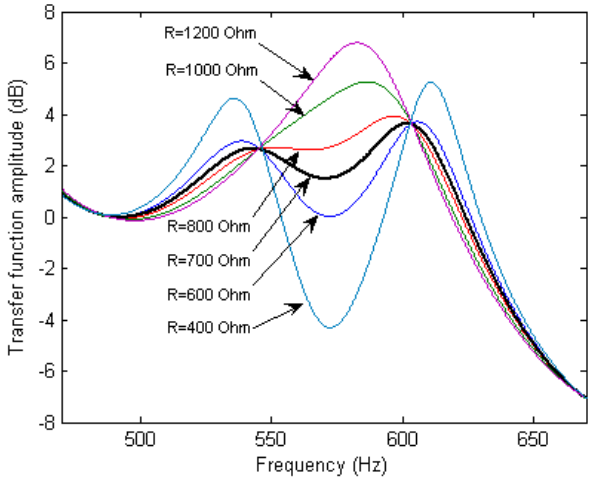

Fig. 6. Uniform beam with different shunt resistances.

Grooving the beam and implementing piezo-electric sensor/actuators introduce a repeating non-uniformity to the beam model, which causes vibration reduction in some frequency bands (stop bands). By tuning the shunt resonance frequencies to different natural frequencies outside stop bands broadband vibration suppression was achieved (see Fig. 7). Tuning frequencies were 4000, 5700, 6700 and 9000 Hz. In all circuits shunt resistance was 100 Ohm. Shunted circuits are accountable for

vibration reduction between 3000 and 11000 hertz while the periodicity caused by installing piezoelectric patches reduced the vibration between 11000 and 16000 hertz. Rotation changes the beam's characteristics natural frequencies. While this change natural frequencies, degrades narrowband vibration suppression, the negative effect of rotation is not severe in broadband vibration suppression (see Fig. 8). For instance, introducing a 50Hz rotation has changed the beam's 9 kHz natural frequency to 9.2 kHz but the vibration is still well damped.

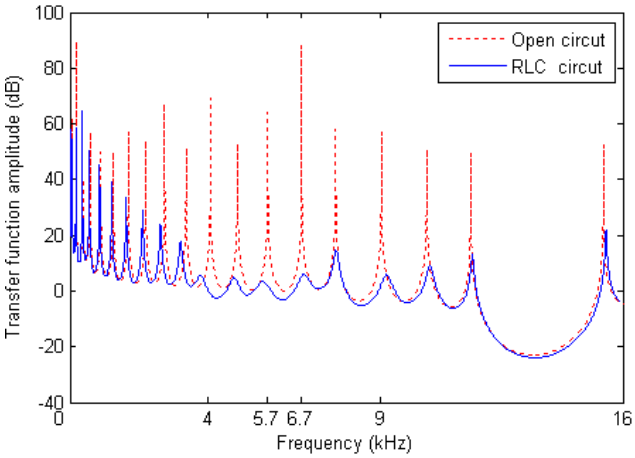

Fig. 7. Vibration attenuation of a non-rotating beam.

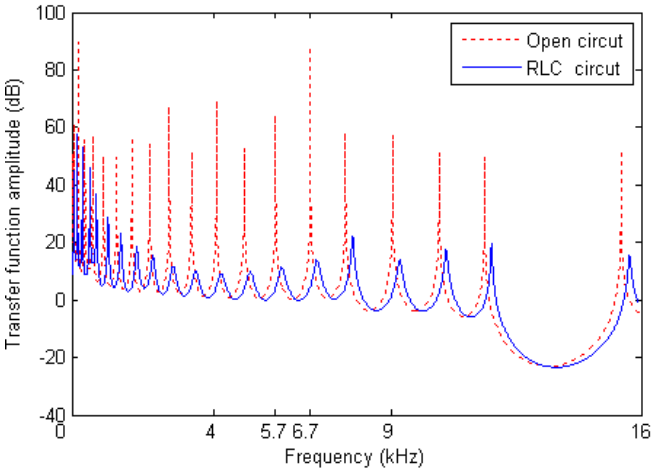

Fig. 8. Vibration attenuation of a rotating beam.

V. Conclusions

In order to attenuate the unwanted vibration in rotating beams over a broad frequency band, a combination of piezo-electric actuators with shunted circuits, and stop bands created by the structure's periodicity was used. The proposed method utilized the beam's periodicity introduced by adding the piezo-electric patches, to attenuate the vibration in high frequencies and piezoelectric patches with shunted circuits to reduce the vibration in mid-frequencies.

In other words, first the piezo-electric patches were added to the beam. This addition created a periodic structure, which significantly reduced the vibration in the high frequency region. Then piezoelectric shunt circuits were implemented and tuned for the mid-frequency range.

Tuning each shunted circuit to a different frequency resulted in vibration reduction in a wide range of frequencies and at the same time reduced the sensitivity of the system to different rotational speeds and therefore eliminated the need for complicated tuning schemes or adaptive shunted circuits.

References

[1] D.D. L., Chung, (2001). Materials for vibration damping: Review, Journal of Materials Science 36, pp. 5733–5737.

[2] R.M., Orris, and M., Petyt, (1974). A finite element study of harmonic wave propagation in periodic structures, J. Sound Vib. 33, pp. 223–36.

[3] I., Shen, (1994). Vibration of Rotationally Periodic Structures. Journal of Sound and Vibration, 459-470.

[4] D., Duhamel, B., Mace, and M., Brennan, (2006). Finite element analysis of the vibrations of waveguides and periodic structures. Journal of Sound and Vibration, 205-220.

[5] F., Romeo, and A., Luongo, (2003). Vibration reduction in piecewise bi-coupled periodic structures. Journal of Sound and Vibration, 601-615.

[6] P., Polach, (2008). Calculation of natural vibration of linear undampoed rotationally periodic structures. Engineering MECHANICS, 15(2), 81-97.

[7] O., Thorp, M., Ruzzene and A., Baz, (2001). Attenuation and localization of wave propagation in rods with periodic shunted piezoelectric patches, Journal of Smart Materials and Structures 10, pp. 979-989.

[8] M., Ruzzene, and A., Baz, (2000). Control of wave propagation in periodic composite rods using shape memory inserts, ASME J. Vib. Acoust. 122, pp. 151–9.

[9] T., Chen, M., Ruzzene, and A., Baz, (2000). Control of wave propagation in composite rods using shape memory inserts: theory and experiments, J. Vib. Control accepted.

[10] N.W., Hagood, and A., von Flotow, (1991). Damping of structural vibrations with piezoelectric materials and passive electrical networks, Journal of Sound and Vibration 146, pp. 243–268.

[11] S.B., Kandagal, S., Sarkar, and K., Venkatraman, (2001). Resonantly shunted piezoelectric layers as passive vibration control devices, Journal of Indian Institute of Science 81, pp. 535-547.

[12] A., Singh, and D., Pines, (2002). Active/Passive Vibration Reduction of Periodic 1-D Structures Using Piezoelectric Actuators. 43rd AIAA/ASME/ASCE/AHS/ASC Structures, Structural Dynamics, and Materials Conference.

[13] J., Tang, and K., Wang, (2004). Vibration Control of Rotationally Periodic Structures Using Passive Piezoelectric Shunt Networks and Active Compensation. J. Vib. Acoust. Journal of Vibration and Acoustics, 379-379.

[14] Kauffman, J., and Lesieutre, G. (2012). Piezoelectric-Based Vibration Reduction of Turbomachinery Bladed Disks via Resonance Frequency Detuning. AIAA Journal, 1137-1144.

[15] W., Zhou, Y., Wu, and L., Zuo, (2014). Cantilever Beam Metamaterial Structure With Periodic Piezoelectric Arrays With High-Order Resonant Circuit Shunts for Vibration Control. Volume 1: Development and Characterization of Multifunctional Materials; Modeling, Simulation and Control of Adaptive Systems; Structural Health Monitoring; Keynote Presentation.

[16] A., Spadoni, M., Ruzzene, and K., Cunefare, (2009). Vibration and Wave Propagation Control of Plates with Periodic Arrays of Shunted Piezoelectric Patches. Journal of Intelligent Material Systems and Structures, 979-990.

[17] J., Becker, M., Maess, O., Fein, L., Gaul, (2006). Finite-element based design of structures with shunted piezoelectric patches for structural vibration damping, Computers and Structures, Vol. 84, Issue 31-32, pp. 2340-2350.

[18] B., Basavaraju Raju, and E., Bianchini, (2005). Improved performance of a baffle-less automotive muffler using piezoelectric materials, Journal of Sound and Vibration, 140, pp. 2347-2353.
[19] O.J., Aldraihem, A., Baz and T.S., Al-Saud, (2007). Hybrid composites with shunted piezoelectric particles for vibration damping, Journal of Mechanics of Advanced Materials and Structures, 14: pp. 413–426.
[20] Sakhaee-Pour, A., Gerami, A. and Ahmadian, A., (2008). Development of an equation to predict radial modulus of elasticity for single-walled carbon nanotubes. Proceedings of the Institution of Mechanical Engineers, Part C: Journal of Mechanical Engineering Science, 222(6), 1109-1115.
[21] Dousti, S., Cao, J., Younan, A., Allaire, P., and Dimond, T., (2012), Temporal and Convective Inertia Effects in Plain Journal Bearings With Eccentricity, Velocity and Acceleration, Journal of Tribology, 134, pp.174-184.
[22] N.W., Hagood, J.B., Aldrich, and A.H., vonFlotow, (1994). "Design of passive piezoelectric damping for space structures", National Aeronautics and Space Administration, Langley Research Center
[23] Dousti, S., (2012), Realistic Squeeze Film Damper Analysis: Application of Gas Turbines Engines, Rotating Machinery and Controls Consortium (ROMAC) Annual Meeting, Charlottesville, VA, USA.
[24] Gerami, A., Allaire, P., and Fittro, R. (2015). Control of Magnetic Bearing With Material Saturation Nonlinearity. Journal of Dynamic Systems, Measurement, and Control,137(6), 061002.
[25] Dousti, S., Dimond, T.W., Allaire, P.E., Wood, H.E., (2013), Time Transient Analysis of Horizontal Rigid Rotor Supported With O-Ring Sealed Squeeze Film Damper, ASME 2013, International Mechanical Engineering Congress and Exposition.
[26] Dousti, S., and Jalali, M.A., (2013), In-Plane and Transverse Eigenmodes of High-Speed Rotating Composite Disks, Journal of Applied Mechanics, 80(1), p.011019.
[27] Gerami, A., Allaire, P., and Fittro, R., (2014). Nonlinear Modeling and Control of a Magnetic Bearing with Material Saturation, Proceedings of the 14th International Conference on Magnetic Bearings, Linz, Austria.
[28] Dousti, S., (2014), An Extended Reynolds Equation Development with Applications to Fixed Geometry Bearings and Squeeze Film Dampers, Ph.D. dissertation, University of Virginia, Charlottesville, Virginia, USA.
[29] Dousti, S., and Fittro, R.L., (2015), An Extended Reynolds Equation Including the Lubricant Inertia Effects: Application to Finite Length Water Lubricated Bearings, Proc. of ASME TurboExpo 2015, GT2015- 43826, June 15-19, 2015, Montreal, Canada.
[30] Dousti, S., (2012), Realistic Squeeze Film Damper Analysis: Application of Gas Turbines Engines, Rotating Machinery and Controls Consortium (ROMAC) Annual Meeting, Charlottesville, VA, USA.
[31] Makhmalbaf, H., Liu, T., and Merati, P., (2015). Experimental Simulation of Buoyancy-Driven Vortical Flow in Jupiter Great Red Spot. Bulletin of the American Physical Society, 60.
[32] Liu, T., Merat, A., Makhmalbaf, M. H. M., Fajardo, C., and Merati, P., (2015). Comparison between optical flow and cross-correlation methods for extraction of velocity fields from particle images. Experiments in Fluids, 56(8), 1-23.
[33] Liu, T., Makhmalbaf, M.H.M., Ramasamy, R.V., Kode, S., and Merati, P., (2015). Skin Friction Fields and Surface Dye Patterns on Delta Wings in Water Flows. Journal of Fluids Engineering, 137(7), 071202.
[34] Makhmalbaf, M.H.M., (2012). Experimental study on convective heat transfer coefficient around a vertical hexagonal rod bundle. Heat and Mass Transfer, 48(6), 1023-1029.
[35] Dousti, S., Gerami, A., Dousti, M., (2016), A Numerical CFD Analysis on Supply Groove Effects in High Pressure, Open End Squeeze Film Dampers, International Journal of Engineering Innovation and Research, 5(1), 80-89.

AUTHOR'S PROFILE

Ali Gerami is a control systems engineer at Wrightspeed, San Jose, California, USA.

Majid Dousti is a research assistant at faculty of engineering, Zanjan University, Zanjan, Iran.

Saeid Dousti is a Senior Technical Fellow at Rotor Bearing Solutions International, Charlottesville, Virginia, USA.